Proceedings of the ASME 2010 3rd Joint US-European Fluids Engineering Summer Meeting and 8th International Conference on Nanochannels, Microchannels, and Minichannels
FEDSM-ICNMM2010
August 1-5, 2010, Montreal, Canada

FEDSM-ICNMM2010-30248

ANALYSIS ON THE STATIC CHARACTERISTICS OF THE NEW TYPE EXTERNALLY PRESSURIZED SPHERICAL AIR BEARINGS

Wang Fusheng
Harbin Institute of Technology
Harbin, Heilongjiang Province, PRC

Bao Gang
Harbin Institute of Technology
Harbin, Heilongjiang Province, PRC

ABSTRACT

The new type externally pressurized spherical air bearings used mass properties measuring instruments are studied which are particularly recommended for determining mass properties of rockets, satellites and ballistic objects. The air bearings are the key component of the mass properties measuring instruments. In order to provide some theoretical guideline for the structure design of the new type externally pressurized spherical air bearings, this paper analyzes static characteristics and the factors affecting the static characteristics of the new type air bearings. A finite volume method is adopted to discretize the three-dimensional steady-state compressible Navier-Stokes equations, and a modified SIMPLE algorithm for compressible fluid is applied to solve the discretized governing equations. The pressure field and velocity field of the air bearings are obtained, from which the carrying capacity, static stiffness and mass flow of the air bearings can be derived, and the factors and rules affecting the static characteristics are analyzed. The calculation method proposed in this paper fits well the general principle, which can be extended to the characteristics analysis of other air bearings.

INTRODUCTION

Air bearings can offer a nearly torque-free environment, perhaps as close as possible to that of space, and for this reason it is the preferred technology for accurate mass properties measurement[1] and ground-based research in spacecraft dynamics and control[2, 3]. Compared with the early adopted orifice compensated air bearings, externally pressurized spherical air bearings have some advantages such simple structure and easy processing. In addition, they are able to ensure the stability in the large scale of pressure[4, 5]. As a result, externally pressurized spherical air bearings have been widely used in mass properties measuring instruments and air bearing spacecraft simulators in recent years.

Mass properties measuring instruments are particularly recommended for determining mass properties of rockets, satellite and ballistic objects. The instruments are capable of high accuracy over a wide range of test object weight and moment of inertia, which permit the measurement of moment of inertia about an axis which does not pass through the center of mass of the test object. The instruments are best made using a system incorporating air bearings to support the test part and define the axis of rotation. And the new type externally pressurized spherical air bearings are the key component of the mass properties measuring instruments. It has been recognized that the spherical air bearings offer the combination of extremely low friction to rotational overturning torque. Willis[6] performed the first investigation of externally pressurized air lubricating films as part of an experimental study of radial air flow between parallel surfaces. Robert L. Grossman[7] studied application of flow and stability theory to the design of externally pressurized spherical gas bearings. GUO, et al[5] and REN, et al[8], studied the static and dynamic characteristics of conventional spherical gas bearings using an finite element method.

This paper emphasizes the research on the new type externally pressurized spherical air bearings used mass properties measuring instruments, aims at analyzing the static characteristics and the factors affecting the static characteristics

of the spherical air bearings. In order to study the static characteristics of the spherical air bearings a calculation method based on three-dimensional model is developed. Due to the complex geometry of the computational domain an unstructured collocated grid technology is used for grid generation in bearings. A finite volume method is adopted to discretize the three-dimensional steady-state compressible Navier-Stokes equations, and a modified SIMPLE algorithm for compressible fluid is applied to solve the discretized governing equations. Upon the completion of the above computation, this paper obtains the pressure field and velocity field of the air bearings, from which the carrying capacity, static stiffness and mass flow of the air bearings can be derived, and analyzing the factors and rules affecting the static characteristics of the spherical air bearings. The research results are expected to be able to provide bases for the structure design of the new type spherical air bearings used mass properties measuring instruments.

THE MODEL OF THE NEW TYPE AIR BEARINGS

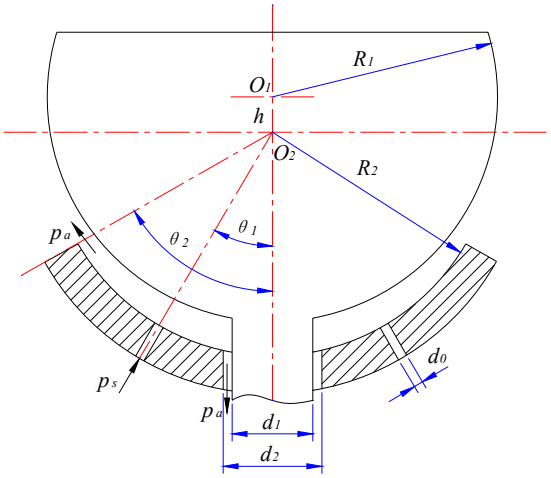

Fig.1 Structure of the new type spherical air bearings

Fig.1 shows the structure of the new type externally pressurized spherical air bearings being studied. Pressurized air from a constant pressure reservoir flows through the orifice into the bearing recess. From the recess the air flows through the clearance space to the rim of the socket and exhausts to the atmosphere. The ball head radius is denoted by R_1 and the ball center is denoted by O_1, whereas R_2 and O_2 refer to the radius and center of the ball socket, respectively. The six proportionally-spaced air intakes have a diameter d_0. The air central outlet of ball socket has a diameter d_2 and the torsion rod connected to ball head has a diameter d_1. The inlet pressure is p_s. After being throttled in the torus formed by the air intake and the air film clearance, the air flow leaves through the air film boundary with the atmospheric pressure p_a. The central air film has the thickness of h. The wrap angle of ball socket corresponding to the air intake is denoted by θ_1, and the wrap angle of ball socket surface is denoted by θ_2.

MESH GENERATION

The six air intakes are evenly distributed along the circumferential direction, and the ball head is not affected by the horizontal force when it is in the float state. Hence, the flow is axis-symmetrical. For air lubrication, the air film thickness is usually tens of microns, which is far smaller than the size of the other two directions, so it leads to the large aspect ratio of the mesh element. In order to reduce the truncation error as well as to avoid numerical divergence, the unstructured hexahedral mesh and pyramid mesh are mainly used in mesh generation. Both the pressure and the velocity vary rapidly around the air intake and the air central outlet of ball socket, for which the structured hexahedral mesh and local mesh refinement method are used. Fig.2 and Fig.3 illustrate the mesh generated in the entire computational domain and a close-up around an air intake, respectively.

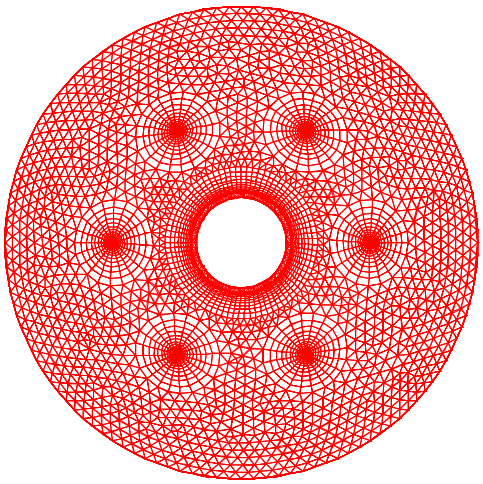

Fig.2 Mesh in the computational domain

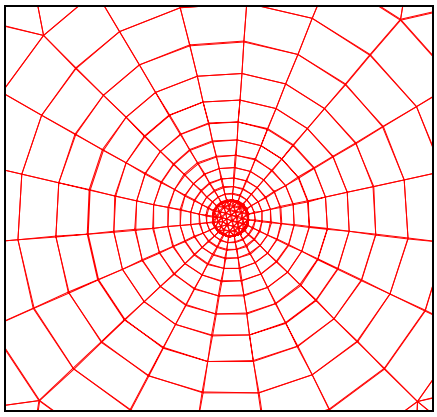

Fig.3 Mesh around an air intake

THE DISCRETIZATION AND SOLUTION OF GOVERNING EQUATIONS

The governing equations for steady-state three-dimensional compressible flows can be found in Ref. [9].

The continuity equation is

$$\mathrm{div}(\rho \boldsymbol{u}) = 0 \tag{1}$$

The momentum equations are as follows:

$$\begin{cases} \mathrm{div}(\rho u \boldsymbol{u}) = \mathrm{div}(\mu \mathrm{grad} u) - \dfrac{\partial p}{\partial x} + S_u \\ \mathrm{div}(\rho v \boldsymbol{u}) = \mathrm{div}(\mu \mathrm{grad} v) - \dfrac{\partial p}{\partial y} + S_v \\ \mathrm{div}(\rho w \boldsymbol{u}) = \mathrm{div}(\mu \mathrm{grad} w) - \dfrac{\partial p}{\partial z} + S_w \end{cases} \tag{2}$$

The energy equation is

$$\mathrm{div}(\rho \boldsymbol{u} T) = \mathrm{div}(\frac{k}{c_p} \mathrm{grad} T) + S_T \tag{3}$$

In order to analyze and solve the above governing equations conveniently, those equations are rewritten in the following general form:

$$\mathrm{div}(\rho \boldsymbol{u} \phi - \Gamma \mathrm{grad} \phi) = S \tag{4}$$

From equation (4), the integral of the general governing equation can be written as follows:

$$\int_{A_{P_0}} (\rho \boldsymbol{u} \phi - \Gamma \mathrm{grad} \phi) \bullet \mathrm{d}\boldsymbol{A} = \int_{V_{P_0}} S \mathrm{d}V \tag{5}$$

For the control volume P_0, equation (5) can be rewritten as follows:

$$\sum_{j=1}^{N} \int_{A_j} (\rho \boldsymbol{u} \phi - \Gamma \mathrm{grad} \phi) \bullet \mathrm{d}\boldsymbol{A} = \int_{V_{P_0}} S \mathrm{d}V \tag{6}$$

where the items of the equation from left to right are convective term, diffusive term and source term.

Discretization of the governing equations

The midpoint rule[10] is adopted in the discretization process to calculate both the surface integral and the volume integral, the former is approximated as the product of the integrand at the cell-face center and the cell-face area, and the latter is approximated as the product of the integrand at the cell-node center and the cell-node volume. Through discretizing the three items given in equation (6), the discretized governing equation for the cell P_0 can be obtained, and the generalized form is

$$a_0 \phi_{P_0} = \sum_{j=1}^{N} a_j \phi_{P_j} + b_0 \tag{7}$$

Under-relaxation method

The under-relaxation technique is usually adopted in the numerical iteration to avoid potential divergence. For the discretized governing equations, the under-relaxation factor can be affiliated directly into the process of solving the algebraic equations, which means that the under-relaxation factor is contained in the main diagonal coefficient of the generated algebraic equations. It is advantageous because of the increased diagonal dominance of the matrix. Therefore, the discrete governing equation given in equation (7) is rewritten as follows:

$$\left(\frac{a_0}{\alpha_\phi}\right) \phi_{P_0} = \sum_{j=1}^{N} a_j \phi_{P_j} + b_0 + \left(\frac{1-\alpha_\phi}{\alpha_\phi}\right) a_0 \phi_{P_0}^0 \tag{8}$$

Boundary conditions

The boundary conditions are implemented in accordance with the following steps:

(1) Let p_i equal to p_s at the pressure inlet.

(2) Let p_i equal to p_a at the pressure outlet.

(3) Let $\partial p_i / \partial n$ equal to zero at the periodic boundary, where n is the surface normal of the periodic boundary.

Solution of governing equations

A modified SIMPLE algorithm suitable for compressible flows is adopted to solve the discretized governing equations. The algorithm can be summarized as follows [11, 12]:

(1) Start the iterative process by guessing the pressure field and density field, which are denoted by p^* and ρ^*, respectively.

(2) Use the values of p^* and ρ^* to solve for u, v and w from the momentum equations. Since these velocities are associated with the values of p^* and ρ^*, they are denoted by u^*, v^* and w^*.

(3) Since they were obtained from guessed values of p^* and ρ^*, the values u^*, v^* and w^*, when substituted into the continuity equation, will not necessarily satisfy that equation. Hence, using the continuity equation, construct a pressure correction p' which when added to p^* will bring the velocity field more into agreement with the continuity equation. That is, the 'corrected' pressure p is

$$p = p^* + p' \tag{9}$$

The velocity corrections u^*, v^* and w^* as well as density correction ρ^* can be obtained from p', then the corresponding corrected items u, v, w and ρ can be obtained as follows:

$$\begin{cases} u = u^* + u' \\ v = v^* + v' \\ w = w^* + w' \end{cases} \tag{10}$$

$$\rho = \rho^* + \rho' \tag{11}$$

(4) Return to step (2), designate the generated values p and ρ as the new values of p^* and ρ^*, and repeat the process until a velocity field is found that dose satisfy the continuity equation.

Analysis of static characteristics

Upon the completion of the above computation, the pressure field and velocity field of the air bearing can be obtained, from which the carrying capacity, static stiffness and mass flow of the air bearings can be derived.

Evaluating the integral of pressure over the upper surface of the air film, the carrying capacity of the air bearing can be determined by

$$W = \left| \int_{A_u} p \mathrm{d}\boldsymbol{A} \right| = \left| \sum_{i=1}^{n} p_i \boldsymbol{A}_i \right| \tag{12}$$

Defining $K_W = \mathrm{d}W/\mathrm{d}h$ as the static stiffness, in order to facilitate the calculation, the finite-difference method is applied to obtain the static stiffness of the air bearing as follows:

$$K_W = \frac{W_h - W_{h-\Delta h}}{\Delta h} \tag{13}$$

Next, the mass flow can be obtained by using the following equation:

$$Q = \int_{A_m} \rho \boldsymbol{u} \cdot \mathrm{d}A = \sum_{i=1}^{m} \rho_i \boldsymbol{u}_i \cdot A_i \tag{14}$$

COMPUTATIONS AND ANALYSIS

Upon the method of the above computation, the bearing capacity, static stiffness and mass flow of the new type externally pressurized spherical air bearings are considered, respectively.

The structural parameters of the air bearings are set as: the ball head radius is R_1=50mm, the ball socket radius is R_2=50mm, the wrap angle of air intake is θ_1=30°, the outer wrap angle of ball socket is θ_2=60°, the number of air intake is 6, and the air intake diameter is d_0=1.2mm. The air central outlet diameter of ball socket is d_2=10mm and the torsion rod diameter connected to ball head has is d_1 =9mm. The air parameters are set as follows: the ambient temperature is T=20 ℃, the ambient pressure is standard atmospheric pressure, the air density is ρ_a=1.226 kg/m^3, and the air dynamic viscosity is μ=1.833×10^{5}Pa•s. The mesh parameters are set as: the number of points around the air outlet is 180, the number of points along the air film thickness direction is 20, and the total number of the meshes is 338 thousand.

The pressure distribution of bearings

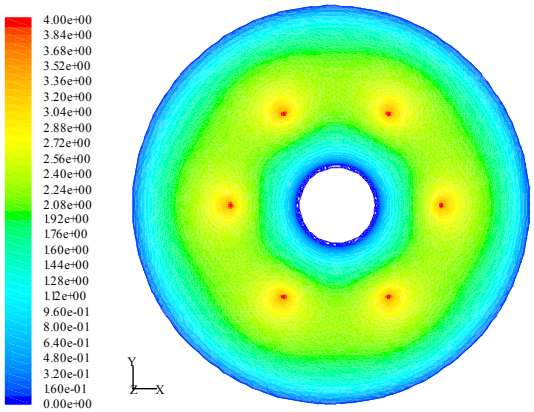

Fig.4 Pressure distribution of spherical gas bearing

When the air supply pressure is 0.4MPa and central air film thickness is h = 20μm, the pressure distribution of the new type externally pressurized spherical air bearings is shown in Fig.4. It can be seen that the pressure of near air intake is maximum, which can reach above 85% of air supply pressure. The pressure of circumference located in air intake is basically the same, which is about 60% of air supply pressure. Due to the second closure affect of air outlet, the pressure on the inner side and outer side of circumference located in air intake is relatively slow, and the pressure reaches 50% of air supply pressure.

When the central air film thickness is 20μm, the Pressure distributing of across air intake along radial axis of spherical air bearings is shown in Fig.5.It can be seen that after air outflows from the air intakes, there is a pressure steep fall around the air intakes. This is due to the existence of air film, the size of throttle surface increasing, and the throttle effect reducing, resulting in the pressure steep fall. As the pressure steep fall only exists in the smaller area near air intakes, which has little effect on bearing capacity.

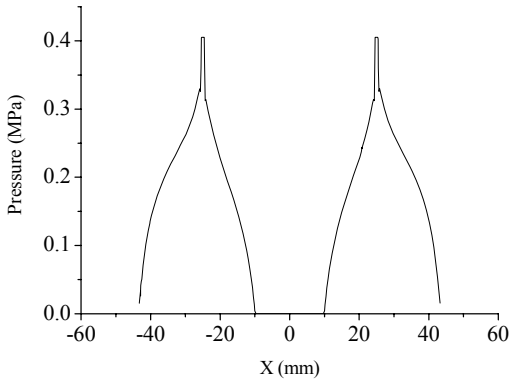

Fig.5 Pressure distributing of across air intake along radial axis

Bearing capacity

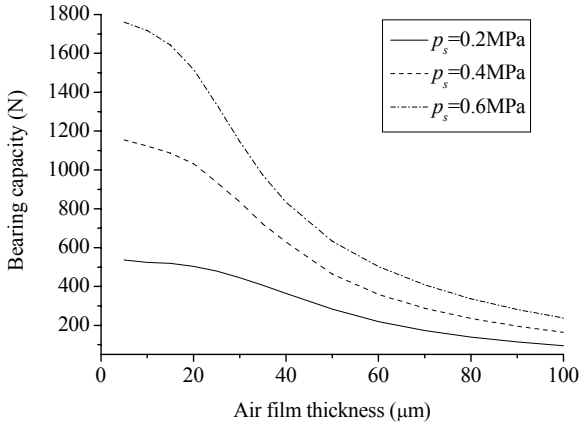

Fig.6 Bearing capacity

When the air supply pressure is p_s=0.2MPa, 0.4MPa, 0.6MPa, the capacity of the new type externally pressurized spherical air bearings varying with central film thickness is shown in Fig.6. It can be seen that the bearing capacity gradually decreases as the central air film thickness increases. For the same central air film thickness, the increasing of air supply pressure results in the increase of the bearing capacity, and the bearing capacity and the air supply pressure is

approximately linearity. Therefore, for the same spherical air bearing, reducing the central air film thickness or increasing air supply pressure can increase its bearing capacity.

Static stiffness

When the air supply pressure is p_s=0.2MPa, 0.4MPa, 0.6MPa, the static stiffness of spherical air bearings varying with central film thickness is shown in Fig.7. It can be seen that for the same air film thickness, the higher air supply pressure, the greater the static stiffness of spherical air bearings. As the air supply pressure increases from 0.2MPa to 0.6MPa, the maximum static stiffness increases from 8.26N/μm to 36.4N/μm. The increasing of static stiffness is very obvious. Therefore, in order to improve the static stiffness of spherical air bearings, it is the most effective means to increase the air supply pressure on the premise of ensuring the bearings stability. Under the different air supply pressure, the corresponding central air film thickness for the maximum static stiffness of spherical air bearings can be changed. As the air supply pressure is p_s=0.2MPa, the corresponding central air film thickness for the maximum static stiffness is 38μm; as the pressure is p_s=0.4MPa, the corresponding central air film thickness for the maximum static stiffness is 30μm; and as the pressure is p_s=0.6MPa, the corresponding central air film thickness for the maximum static stiffness is 24μm.

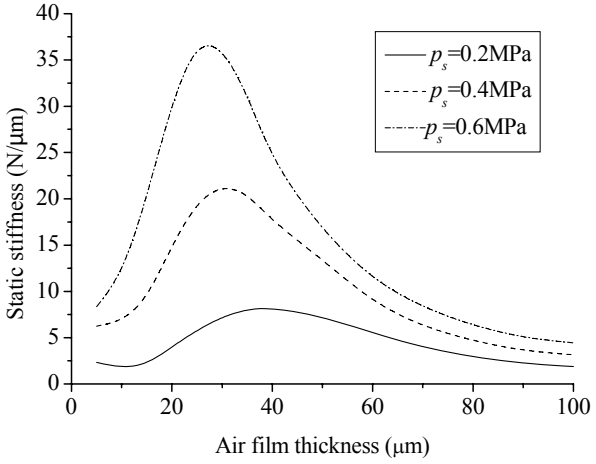

Fig.7 Static stiffness

Mass flow

When the air supply pressure is p_s=0.2MPa, 0.4MPa, 0.6MPa, the mass flow of spherical air bearings varying with central film thickness is shown in Fig.8. It can be seen that for the same air film thickness, the higher air supply pressure, the greater the mass flow of spherical air bearings. And the mass flow is approximately proportional to the air supply pressure. For the same central air film thickness, the mass flow of spherical air bearings increases as the central air film thickness increases. Therefore, for the same spherical air bearing, reducing the air supply pressure or the central air film thickness can reduce the mass flow (air consumption) of the bearing. For the same load (bearing capacity), when the air supply pressure decreases, the central air film thickness reduces, which results in the mass flow decreasing of spherical air bearing.

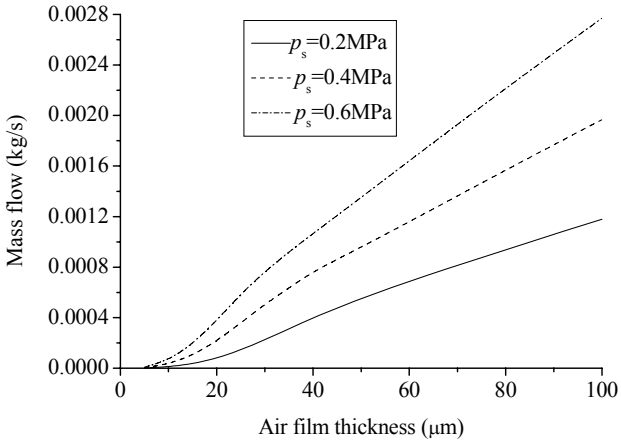

Fig.8 Mass flow

CONCLUSIONS

The new type externally pressurized spherical air bearings being studied in this paper, and the three-dimensional finite volume method is adopted to study the static characteristics of the new type air bearings.

The air supply pressure and central air film thickness have a great influence on the capacity and static stiffness of the new type spherical air bearings. The capacity and static stiffness of the air bearings greatly increase as the air supply pressure increases and the central air film thickness decreases. And for the same load (bearing capacity), when the air supply pressure decreases, the mass flow of new type air bearings reduces as the central air film thickness reduces.

NOMENCLATURE

div(·)	=	divergence operator
ρ	=	air density
$\boldsymbol{u}$	=	velocity vector.
u	=	x axes of the velocity vector
v	=	y axes of the velocity vector
w	=	z axes of the velocity vector
μ	=	dynamic viscosity
p	=	pressure
S_u, S_v, S_w	=	generalized source terms of the momentum equations
T	=	temperature
k	=	heat transfer coefficient
c_p	=	specific heat
S_T	=	viscous dissipation term
ϕ	=	general variable, and the general equation represents the continuity equation, the momentum equations and the energy equation when ϕ is set as 1, u, v, w and the temperature T, respectively

Γ, S = generalized diffusion coefficient and generalized source term

P_0 = control volume

V_{P_0} = volume of P_0

A_{P_0} = surface area of P_0

$\boldsymbol{A}$ = area vector of the control volume interface, which is composed of $\boldsymbol{A}_j$(j=1, 2,⋯ , N). The positive direction of $\boldsymbol{A}_j$ coincides with the unit vector of the surface normal pointing outside, and N equals to 6 and 5 for the hexahedral mesh and the pyramid mesh, respectively

a_0 = center coefficient

a_j = influence coefficient of the adjacent elements

b_0 = constant of the source term

α_ϕ = under-relaxation factor of the variable ϕ

$\phi_{P_0}^0$ = result of ϕ_{P_0} from the last iteration

A_u = upper surface area of the air film

A_i = area vector of the ith mesh

n = number of the meshes on the upper surface of the air film

Δh = calculation step with respect to the central air film thickness, which is set as 0.5μm in this paper

A_m = area of the air intake, and m denotes the number of the meshes on the air intakes

REFERENCES

1 Richard Boynton, Kurt Wiener. A New High Accuracy Instrument for Measuring Moment of Inertia and Center of Gravity. The 47th Annual Conference of the Society of Allied Weight Engineers, SAWE PAPER No 1827, 1988.

2 SCHWARTZ J L, PECK M A, HALL C D. Historical review of air-bearing spacecraft simulators. Journal of Guidance, control, and Dynamics, Vol.26, No.4, 2003, pp.513-522.

3 Richard Boynton. Using a Spherical Air Bearing to Simulate Weightlessness. The 55th Annual Conference of the Society of Allied Weight Engineers, SAWE PAPER No.2297, 1996.

4 Du Jinming, Lu Zhesheng, Sun Yazhou. Comparison of all types of restriction for aerostatic bearings. Aviation Precision Manufacturing Technology, Vol.39, No.6, 2003, pp.4-7. (in Chinese)

5 Guo Liangbin, Wang Zuwen, Bao Gang, et al. Finite element analysis the dynamic characteristics of static pressure spherical air bearings with inherent compensation. China Mechanical Engineering, Vol.15, No.23, 2004, pp.2069-2073. (in Chinese)

6 Willis, Rev. R. On the pressure produced on a flat plate when opposed to a stream of air issuing from an orifice in a plane surface. Trans Cambridge Phil Soc. Vol.3, No.1, 1828, pp.121-140.

7 Robert L. Grossman. Application of flow and stability theory to the design of externally pressurized spherical gas bearings. Journal of Basic Engineering, Dec, 1963, pp.495-502.

8 Ren Di, Wang Zuwen, Yang Qingjun, et al. Effect of manufacturing errors on static characteristics of externally pressurized spherical air bearings. Chinese Journal of Mechanical Engineering. Vol.22, No.5, 2009, pp.896-902.

9 VERSTEEG H K, MALALASEKERA W. An introduction to computational fluid dynamics: The finite volume method. Upper Saddle River, New Jersey: Prentice Hall, 2007.

10 FERZIGER J H, PERIC M. Computational methods for fluid dynamics. Berlin: Springer-Verlag, 2002.

11 RHIE C M, CHOW W L. A numerical study of the turbulent flow past an isolated airfoil with trailing edge separation. AIAA J., Vol.21, No.11, 1983, pp.1 525–1 532.

12 PRZULJ V, BASARA B. A simple-based control volume method for compressible flows on arbitrary grids. AIAA Paper 2002-3289, 2002.